Translational Oncology 15 (2022) 101279

Contents lists available at ScienceDirect

Translational Oncology

journal homepage: www.elsevier.com/locate/tranon

Original Research

Combined multimodal ctDNA analysis and radiological imaging for tumor surveillance in Non-small cell lung cancer

Martin Metzenmacher [a,b], Balazs Hegedüs [c], Jan Forster [e,d], Alexander Schramm [f], Peter A. Horn [g], Christoph A. Klein [h,i], Nicola Bielefeld [d,j,k], Till Ploenes [c], Clemens Aigner [c], Dirk Theegarten [l], Hans-Ulrich Schildhaus [l], Jens T. Siveke [d,j,k], Martin Schuler [a,b,d], Smiths S. Lueong [d,j,k,*]

[a] Department of Medical Oncology, West German Cancer Center, University Hospital Essen, University Duisburg-Essen, Hufelandstrasse 55, Essen 45122, Germany
[b] Division of Thoracic Oncology, West German Cancer Center, University Medicine Essen-Ruhrlandklinik, University Duisburg-Essen, Tüschener Weg 40, Essen 45239, Germany
[c] Department of Thoracic Surgery, West German Cancer Center, University Medicine Essen Ruhrlandklinik, University Duisburg-Essen, Essen D-45239, Germany
[d] German Cancer Consortium (DKTK), Partner site University Hospital Essen, Hufelandstrasse 55, Essen 45122, Germany
[e] Chair for Genome Informatics, Department of Human Genetics, University Hospital Essen, University Duisburg-Essen, Hufelandstrasse 55, Essen 45122, Germany
[f] Laboratory for Molecular Oncology, Department of Medical Oncology, West German Cancer Center, University Hospital Essen, University of Duisburg-Essen, Essen 45122, Germany
[g] Institute for Transfusion Medicine, University Hospital Essen, Essen 45122, Germany
[h] Experimental Medicine and Therapy Research, University of Regensburg, Regensburg 93053, Germany
[i] Fraunhofer-Institute for Toxicology and Experimental Medicine, Division of Personalized Tumor Therapy, Regensburg 93053, Germany
[j] Institute for Developmental Cancer Therapeutics, West German Cancer Center, University Hospital Essen, Essen 45122, Germany
[k] Division of Solid Tumor Translational Oncology, German Cancer Consortium (DKTK, partner site Essen) and German Cancer Research Center, DKFZ, Heidelberg, Germany
[l] Institute of Pathology, University Hospital Essen, Essen, Germany

ARTICLE INFO

Keywords:
Lung cancer
ddPCR
NGS
cfDNA methylation
Surveillance

ABSTRACT

Background: Radiology is the current standard for monitoring treatment responses in lung cancer. Limited sensitivity, exposure to ionizing radiations and related sequelae constitute some of its major limitation. Non-invasive and highly sensitive methods for early detection of treatment failures and resistance-associated disease progression would have additional clinical utility.

Methods: We analyzed serially collected plasma and paired tumor samples from lung cancer patients (61 with stage IV, 48 with stages I-III disease) and 61 healthy samples by means of next-generation sequencing, radiological imaging and droplet digital polymerase chain reaction (ddPCR) mutation and methylation assays.

Results: A 62% variant concordance between tumor-reported and circulating-free DNA (cfDNA) sequencing was observed between baseline liquid and tissue biopsies in stage IV patients. Interestingly, ctDNA sequencing allowed for the identification of resistance-mediating p.T790M mutations in baseline plasma samples for which no such mutation was observed in the corresponding tissue. Serial circulating tumor DNA (ctDNA) mutation analysis by means of ddPCR revealed a general decrease in ctDNA loads between baseline and first reassessment. Additionally, serial ctDNA analyses only recapitulated computed tomography (CT) -monitored tumor dynamics of some, but not all lesions within the same patient. To complement ctDNA variant analysis we devised a ctDNA methylation assay (^{meth}cfDNA) based on methylation-sensitive restriction enzymes. cfDNA methylation showed and area under the curve (AUC) of > 0.90 in early and late stage cases. A decrease in ^{meth}cfDNA between baseline and first reassessment was reflected by a decrease in CT-derive tumor surface area, irrespective of tumor mutational status.

* Corresponding author at: Bridge Institute for Experimental Cancer Therapy and German Consortium for Translational Cancer Research (DKTK), Partner site University Hospital Essen, West German Cancer Center, Hufelandstrasse 55, Essen 45147, Germany.

E-mail addresses: Martin.Metzenmacher@uk-essen.de (M. Metzenmacher), Balazs.Hegedues@rlk.uk-essen.de (B. Hegedüs), j.forster@dkfz-heidelberg.de (J. Forster), alexander.schramm@uni-due.de (A. Schramm), Peter.Horn@uk-essen.de (P.A. Horn), Christoph.Klein@klinik.uni-regensburg.de (C.A. Klein), Nicola.Bielefeld@uk-essen.de (N. Bielefeld), Clemens.Aigner@rlk.uk-essen.de (C. Aigner), Jens.Siveke@uk-essen.de (J.T. Siveke), Martin.Schuler@uk-essen.de (M. Schuler), smiths-sengkwawoh.lueong@uk-essen.de (S.S. Lueong).

https://doi.org/10.1016/j.tranon.2021.101279
Received 29 July 2021; Received in revised form 27 October 2021; Accepted 28 October 2021

Conclusion: Taken together, our data support the use of cfDNA sequencing for unbiased characterization of the molecular tumor architecture, highlights the impact of tumor architectural heterogeneity on ctDNA-based tumor surveillance and the added value of complementary approaches such as cfDNA methylation for early detection and monitoring

Introduction

Lung cancer, predominantly non-small cell lung cancer (NSCLC), is one of the leading causes of cancer-related deaths and contributes substantially to the global cancer burden [1,2]. During the past decade, therapeutic advances have improved patient survival. However, the 5-year survival rate is still unacceptably poor [3].

When diagnosed at an early stage, NSCLC treatment relies on curative intent surgery [4,5] or multimodal treatment with radiotherapy and surgery [6–8]. Surgery-ineligible patients receive palliative systemic therapies [6–8]. Platinum-based chemotherapy combined with PD-(L)1 checkpoint-inhibition is the standard of care for the majority of patients [6–8], meanwhile tyrosine kinase inhibitors (TKIs) are used for patients with actionable mutations [7,8]. Irrespective of the systemic treatment modality, most patients eventually develop resistance-mediated disease progression. This particularly raises an unmet need for tools that can allow for monitoring biological disease progression.

Radiological imaging is the established standard of care for disease surveillance in most tumor diseases. These procedures however come with the burden of exposure to ionizing radiation and related sequelae. Furthermore, only visible increases in tumor mass can be assessed. To prevent exposure to ineffective and potentially toxic therapies, alternative tools for monitoring disease progression needs to be developed to detect biological disease progression in a timely manner [8].

From current understanding, NSCLCs are driven by activating mutations of proto-oncogenes such as *EGFR, KRAS, BRAF, PIK3CA* as well as translocations in the *ALK* and *ROS1* genes. Frequently, this coincides with inactivating mutations in tumor suppressors such as tumor protein 53 (*TP53*) [9,10]. Tumor-derived actionable alteration in *EGFR, ALK* and *ROS1* license patients for TKI administration and improves progression-free survival [11]. However, tumor-derived DNA mutation scoring is difficult to implement in all patients [12,13,14]. Architectural differences in tumor clonal composition are not accounted for by tumor biopsies and multiple lesions from the same patient are difficult to sample in this manner. To monitor cancer evolution under the selective pressure of a given treatment, repeated biopsies are required, which suffer the same risks and restrictions. Circulating cell-free DNA analysis can allow for noninvasive longitudinal tumor interrogation for clinically relevant alterations [15,16]. Mutation analysis as well as methylation analysis on circulating DNA has been reported in solid tumors [17,18]. In effect, circulating tumor DNA and cell-free DNA methylation analyses have been shown to have promising potentials for disease detection and surveillance in several tumor entities [19,20]. Pan-cancer analyses of cell-free circulating DNA revealed the presence of circulating tumor DNA in several solid tumors irrespective of disease stage [21]. Interesting, cfDNA methylation has recently been reported to be very promising for early detection and of different cancer types and patient stratification [22,23]

Herein, we report on combined multimodal analysis of circulating cell-free DNA (cfDNA) and radiological imaging for detection and monitoring of NSCLC. We show that ctDNA anaylsis by next-generation sequencing (NGS) and droplet digital PCR (ddPCR) for single nucleotide variations (SNVs) can allow for disease detection and treatment monitoring but is limited by tumor cell clonal heterogeneity. This limitation can be compensated for by our cfDNA methylation assay. We further show that ultra-deep ctDNA sequencing identifies resistance-mediating alterations in cfDNA from treatment-naïve samples and thus highlight the role of tumor architecture and heterogeneity on patient outcome.

Methods

Patient cohorts

Patients included in this study were prospectively recruited at the outpatient unit of the Department of Medical Oncology at the West German Cancer Center, University Hospital Essen (stage IV) or at the Department of Thoracic Surgery at the Ruhrlandklinik (stage I–III). Stage IV patients were included if they had only lung cancer, gave consent for the use of their samples for molecular analyses and there was available tumor tissue as fresh frozen or formalin-fixed paraffin-embedded tissue. Stage I-III patients were equally included, if they had clinically confirmed non-metastatic lung cancer and were eligible for curative intent surgery. Healthy blood samples were collected from transfusion blood donors at the Department of Transfusion Medicines at the University Hospital in Essen. The local institutional review boards approved the study (17–7740-BO, 14–6056-BO, 14–5961-BO and 17–7729-BO). All participants provided written informed consent.

Blood sampling and radiological assessments

A volume of 7.5 ml of blood was drawn into EDTA blood tubes (ref # 01.1605.001, Sarstedt, Nümbrecht, Germany) at between 0 and 2 weeks before the start of systemic treatment or before surgery. Serial blood collection and CT-based response evaluation was organized during each treatment cycle for patients receiving systemic therapy. Plasma was prepared by a three-step centrifugation at 4 °C and tumor response was evaluated using RECIST 1.1. Furthermore, treatment-naïve tumor biopsies or surgical material were available from all patients as formalin-fixed paraffin-embedded (FFPE) sections. The duration between tumor sampling and blood sampling was less than 10 days.

DNA isolation and ctDNA measurement by ddPCR

cfDNA isolation was performed on a Maxwell system (Promeg Corporation, Madison, USA) following manufacturer's instructions. Circulating levels of ^{mut}*KRAS (Codon 12/13),* ^{mut}*BRAF* (V600E) and ^{mut}*EGFR* (L858R) were measured by means of ddPCR using ddPCR mutation detection assays for the target variants (Bio-Rad, California, USA). All reactions were performed in 20 µl reactions in duplicates using 5 µl of cfDNA from each sample and data expressed per ml of plasma used. The reaction was performed using the QX100™ ddPCR system (Bio-rad). After droplet generation, the PCR reaction was performed in a T100^{Tm} thermocycler (Bio-rad). The following cycling conditions were used: 95 °C for 10 min, followed by 40 cycles of 95 °C for 30 s and 55 °C for 1 min at a ramp rate of 2 °C/sec and then 1 cycle at 98 °C for 10 min and the reaction held at 4 °C until droplets were analyzed

DNA isolation from FFPE material

One tumor-rich block based on the evaluation of the H&E slides was selected from each case. Five 5 µM sections were collected in a tube and DNA was extracted using the QIAamp DNA FFPE Tissue Kit (Qiagen, Hilden, Germany) following the manufacturer's protocol. DNA concentration was measured with Qubit 3.0 (Life Technologies, Carlsbad, CA, USA).

In silico data mining

Microarray methylation expression was downloaded from array express GSE66836 and GSE83842. Database mining was performed in the R environment. The first data set (GSE66836) was derived from non-small cell lung cancer tumor samples at different stages as well as paired adjacent non-tumor lung and served as a discovery cohort. We then used a second dataset (GSE83842), as a validation, to make sure that the methylations events observed were independently reproducible. Additionally, the second dataset was used because it was made up of only localized tumors (stage I) tumors and adjacent non-tumor lung tissue. The methylation events observed in this dataset could therefore further be investigated as potential markers for early detection

DNA sequencing an data analysis

DNA sequencing analyses was parformed using an in-house clinically relevant custom Generead (Qiagen, Hilden, Germany) panel for tumor tissue, while the Avenio ctDNA targeted kit (cat # 08,061,068,001, Roche, Indianapolis, USA) was used for plasma-derive DNA sequencing. All samples analyzed on the avenio platform had atleast one tumor-reported genetic alteration covered by the Avenio ctDNA targeted panel. DNA sequencing libraries were prepared from 20 ng of covaris-fragmented FFPE-derived tumor DNA or directly from 10 ng of cfDNA. cfDNA libraries were generated using the AVENIO targeted panel following manufacturer's instructions and sequenced 100 bp PE on a HiSeq 4000. A clinically relevant custom Generead targeted parnel was used to generate tumor DNA libraries using the NEBNext Ultra DNA library prep kit for illumina (New England Biolabs) and sequenced 150 bp PE on a Miseq. The AVENIO data was analyzed using the proprietary Avenio oncology analysis software (2.0) while the Generead panels were analyzed using the Cancer Research Workbench (CLC Bio 21. 0. 5, Qiagen, Hilden Germany). Gene translocations were analyzed in tumor tissue by means of the ZytoLight ® SPEC RET Dual Color Break Apart Probe (cat # Z-2148–200, Zytovision, Bremerhaven, Germany).

DNA methylation analysis

Given that even the Avenio platform did not find all tumor-reported mutations in baseline cf DNA samples, we therefore sort to develop a complementary approach for the assessement of tumor dynamics in patients without any actionable mutations. This will allow for broadening the spectrum of patients who can be analyzed by minimally invasive approaches such as liquid biopsies. To this end, we developed a methylation-sensitive restriction enzme- based cfDNA methylation assay. This assay is less aggressive compared with the conventional bisulfite conversion and can provide data at single nucleotide resolution. Restriction digestion was performed with 10 ng of cfDNA and 25 ng of tumor DNA using 20 units of the restriction enzyme BspT104I (Takara Bio) overnight at 37 °C. For ddPCR, 5 µl of the digested product was used and DNA methylation was measured using the ddPCR master mix for probes without dUTP (Bio-rad) in a total reaction volume of 20 µl. The cycling conditionas were as follows: 95 °C for 10 min, followed by 40 cycles of 95 °C for 30 s and 60 °C for 1 min at a ramp rate of 2 °C/sec and then 1 cycle at 98 °C for 10 min and the reaction held at 4 °C until droplets were analyzed. The primer sequencesused were: cg7111-Fow 5′- GTAGGCGTTCTTTCCTG-3′ and cg7111-rev 5′- GAATTGAAGTGGCGAAGAC-3′ and the detection probe used was HEX-CGAGCCCTTCGAACTCTCG-BBQ. Raw counts were then expressed per ml of plasma or per ng for the tumor DNA.

Statistical analysis

Students' *t*-test was used to compare the mean of two groups. The strength of relationship between ^{met}cfDNA concentration and ddPCR-detected copies per ml was assessed by Pearson correlation. Statistical significance was set to a p value < 0.05. The diagnostic performance of the marker was evaluated with the ROCR package [24]. Data analysis was performed in the R version 3.6-environment and Graphpad Prism version 7.0 (GraphPad Software, Inc, La Jolla California USA). Progression-free survival was defined as the time from treatment initiation until clinical disease progression or progression-associated death

Results

Samples and analyses

Three sample cohorts were analyzed in the present study (Fig. 1). The control cohort had 39 healthy transfusion blood donors and 22 non-tumor fresh frozen lung tissues. The early stage cohort was composed of 48 paired FFPE tumor tissue/preoperative plasma samples. The control and early stage cohorts were analyzed for DNA methylation . Of 70 cases in the advanced stage cohort, 61 samples were analyzed by panel sequencing of tumor DNA or fluorescent *in situ* hybridization. Patient baseline characteristics are shown in **Supplementary Table 1.** All 61 stage IV cfDNA samples were equally analyzed for methylation. cfDNA sequencing was performed on 16 baseline samples from advanced stage cases while serial analyses of 13/16 plasma samples was achieved for hotspot loci by ddPCR. Longitudinal methylation analysis was performed on 17 patients (40 samples).

Targeted analyses of paired tumor- and plasma–derived DNA

We analyzed 46 treatment-naïve tumor biopsies from stage IV NSCLC patients using a clinically relevant custom Generead version 2 (Qiagen GmbH, Hilden, Germany) targeted panel comprising 239 amplicons and spanning 20 Kb while 15 were analyzed by FISH. Baseline cfDNA from 16 of these patients was analyzed on the AVENIO platform (Roche Diagnostics Mannheim, Germany). Using ddPCR, hotspot loci were analyzed in the *BRAF* (V600E), *KRAS* (Codon 12/13) and *EGFR* (L858R) gene loci in 13/16 samples.

In tumor tissue, single nucleotide variations were most frequent 58/79 (73.4%). Deletions represented 7.6% (6/79) of all alterations while translocations accounted for 10.1% (8/79) of all alterations. As seen from Fig. 2**a**, *TP53, KRAS* and *EGFR* were the most mutated genes in tumor samples, meanwhile other less frequent mutations were observed on other genes such as *PIK3CA, BRAF* and *STK11*. Furthermore, there were other genomic alterations such as *MET* and *ERBB2* amplifications as well as *ALK, ROS1* and *RET* translocations. *ALK, ROS1* and *RET* translocations were observed in 8%, 4% and 4% of patients, respectively after FISH analysis. Low-level amplifications were observed in the *MET* and *ERBB2* gene loci (Fig. 2**a**). Similar mutation patterns have been observed in other studies [25].

In cfDNA, we identified more somatic variants compared with the corresponding tumor samples using the AVENIO platform. All of these alterations were single nucleotide variations. All samples selected for ctDNA analysis had at least one tumor-confirmed somatic variant covered by the AVENIO targeted panel. ctDNA, mutations were most frequently identified in the *EGFR* (88%), *ROS1* (88%), *BRCA1* (81%) *ERBB2* (62%) and *TP53* (62%) gene loci. Other less frequently mutated genes in cfDNA were: *BRAF, BRCA2, PDGFRA, BRAF, KIT* and *KRAS* (Fig. 2**b**). Interestingly, in one baseline cfDNA sample, we identified a p. T790M mutation, which was not detected in the corresponding tumor tissue. We investigated the agreement in variant calls obtained from tumor tissue and baseline cfDNA from the same patient. To this end, we matched tumor- and cfDNA-derived calls from each of the 16 patients analyzed on both platforms. A patient was concordant, if at least one identical call was observed in tumor- and plasma-derived DNA from the different platforms. A concordance in 62% of patients was observed between baseline cfDNA and tumor DNA sequencing (Fig. 2**c**). Of the 13 samples cfDNA analyzed by ddPCR, tumor-reported variants could be identified in a total of 9 samples (9/13), resulting in a concordance rate

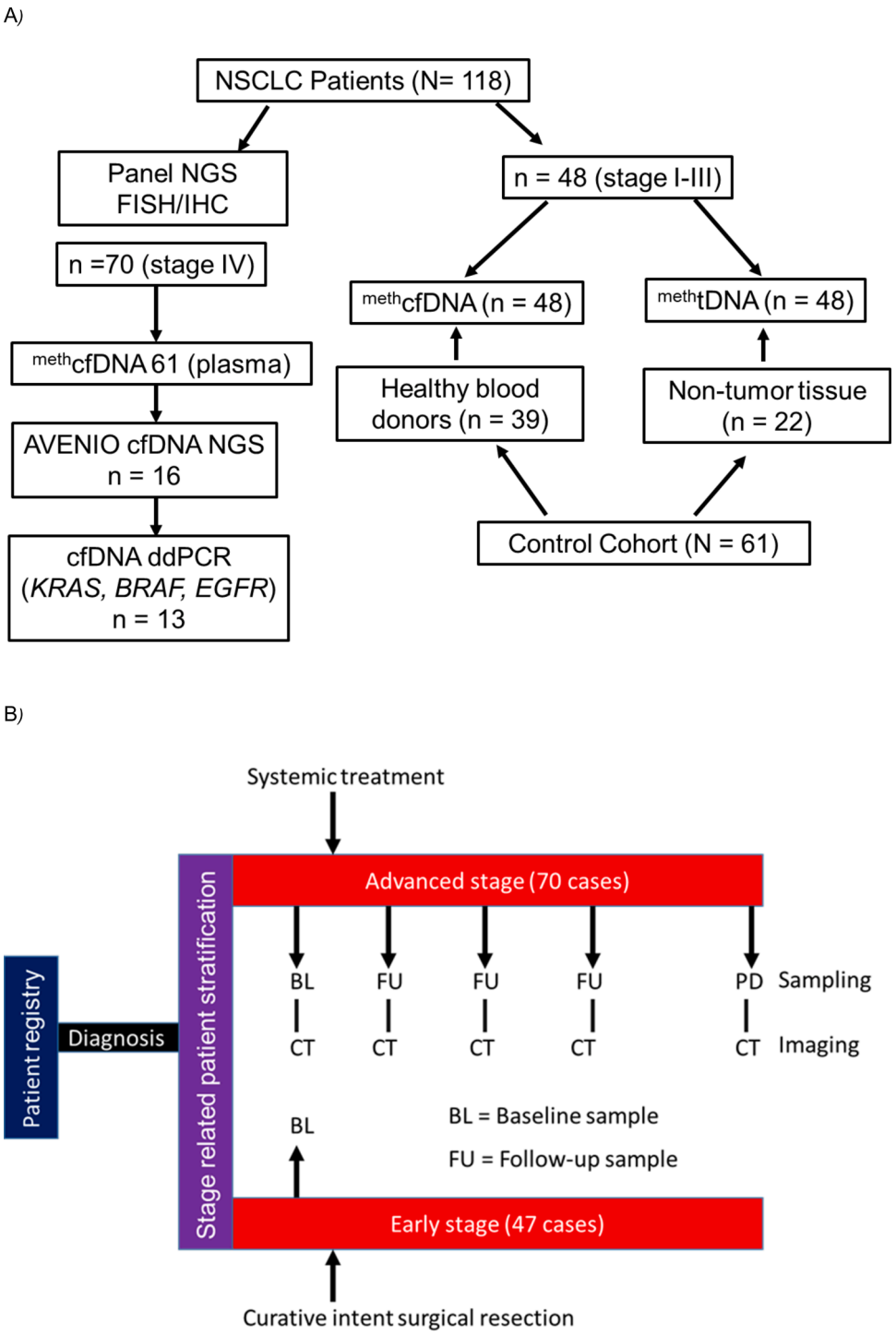

Fig. 1.. CEVIR project design. (A) A consort diagram showing different patient cohorts and analyses performed. (B) Patient recruitment and sampling plan within the CEVIR study.

of 69%. Specifically, all 2/2 *BRAF* tumor variants were detected while 2/4 *EGFR* (L858R) mutations could be confirmed. In the *KRAS* locus, 5/7 samples were positive. (Fig. 2**d**). A summary of all mutations detected in plasma by the Avenio panel are given in **Supplementary Table 1**.

Monitoring treatment response in ctDNA by ddPCR

We analyzed baseline and post treatment samples from 13 patients bearing *KRAS* (codon 12/13), *BRAF* (V600E) and *EGFR* (L858R) mutations by ddPCR. Irrespective of gene locus, ctDNA concentrations decreased in 12/13 cases in post-treatment samples (Fig. 2**d**). Radiological imaging data from these patients was analyzed at the plasma sampling time points. In three patients with different clinical profiles and bearing mutations in the *KRAS, BRAF* and *EGFR* loci, representative patient profiles are shown (Fig. 3). In the patient with a mutant *KRAS* tumor, (^{mut}*KRAS)* (patient #1) with two metastatic lesions, ctDNA kinetics completely reflected the pattern of tumor dynamics of both lesions (Fig. 3**a–c**). In effect, when the normalized ctDNA concentration increased, there was a corresponding increase in the tumor surface area. Similarly, when there was a decrease in the ctDNA concentration, the

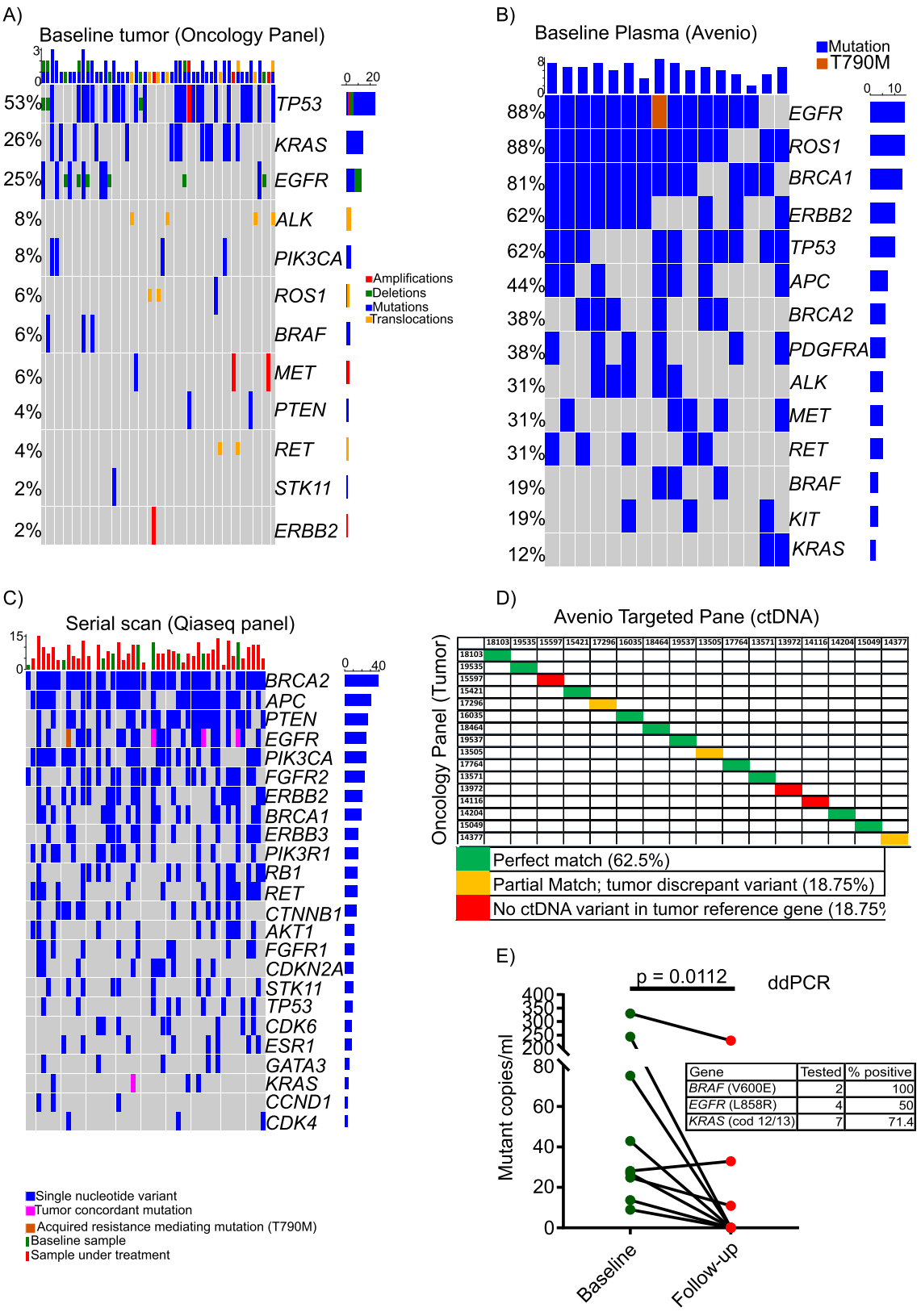

Fig. 2.. Ultra-deep cfDNA sequencing partially recapitulates tumor genomics landscape and reveals tumor architectural discrepancies. (**A**) An oncoprint of the molecular alterations identified in patient tumors biopsies. Only clinically relevant and tumor-driving alterations are shown. (**B**) Oncoprint showing the molecular alterations in cfDNA from first 16 patients selected from the tumor data (AVENIO). (**C**) An oncoprint showing the molecular evolution of ctDNA before and during treatment (green =baseline and red = under treatment) (**D**) A concordance matrix showing the concordance between tumor-derived variants and cfDNA-derived variants from the same patients. (**E**) A profile plot showing ctDNA dynamic between baseline and first reassessment. (For interpretation of the references to color in this figure legend, the reader is referred to the web version of this article).

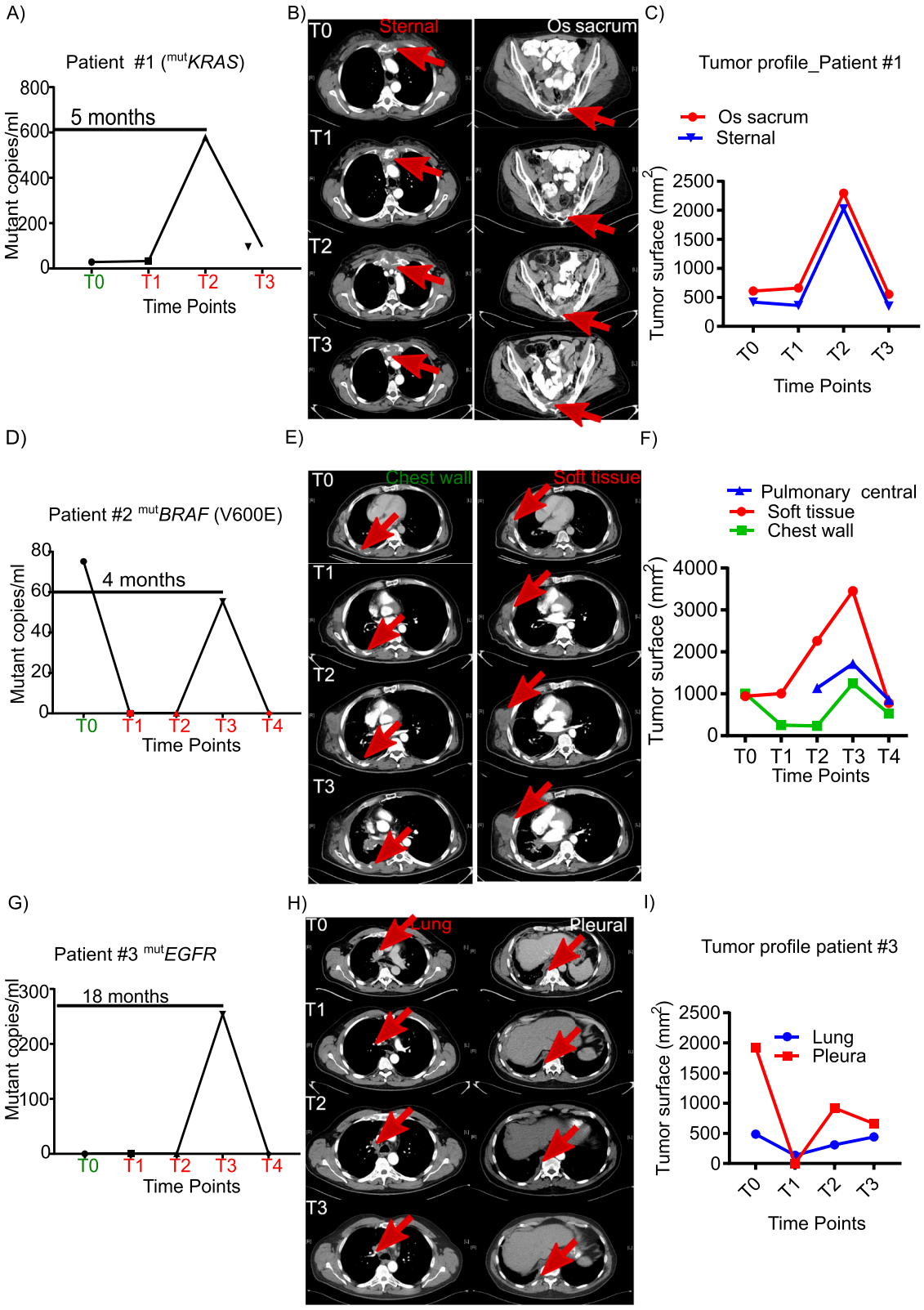

Fig. 3.. Serial ctDNA monitoring allows for response monitoring in the source clone.(A) A profile plot for [a] mut*KRAS* tumor showing mut*KRAS* profile before treatment (green) and during treatment (red). (B) CT images of metastatic lesion in mut*KRAS* patient. (C) Tumor surface area profile of individual lesions mut*KRAS* tumor. (D) A profile plot for a mut*BRAF* (V600E) patient showing ctDNA profile before (green) and during treatment (red). (E) CT images of individual lesion in mut*BRAF* tumor. F) Representative tumor surface area profile of some lesions in mut*BRAF* tumor. (G) A profile plot for a mut*EGFR* mutant tumor showing ctDNA before treatment (green) and during treatment (red). (H) CT images of lung and pleural lesions in mut*EGFR* patient. (I) Tumor surface area profile of all lesions in the patient. (For interpretation of the references to color in this figure legend, the reader is referred to the web version of this article).

tumor surface area decreased. In the patient with a mutant *BRAF* tumor (patient #2) there were three metastatic lesions (soft tissue, chest wall and the central pulmonary). The ctDNA kinetics reflected the patterns of the tumor dynamics corresponding to the chest wall lesion only (Fig. 3**d–f**). A third patient with ^{mut}*EGFR* mutant tumor (patient #3) had a lung and a pleural lesion. ctDNA kinetics showed a closer profile to the lung lesion alone as seen in the CT-scan and tumor surface area (Fig. 3**g–i**).

MSRE-ddPCR for quantification of CPG methylation status

We analyzed two 450k methylation data sets (GSE66836 & GSE 83,842) and identified 111 (Supplementary Table 2) hyper-methylated CpG sites carrying restriction sites (**Supplemental Fig. 1 and Supplementary Table 3**). We selected a smoking- and stage-independent hypermethylated CpG locus for assay development and testing. The CpG (cg03287111) is located on the *GLI2* gene body on chromosome chr2:121,625,484–121,625,784. This CpG position was chosen because it was not stage-specific or age-related and was hyper methylated in both advanced and early stage cases. It could therefore be further developed for early detection or screening of high risk populations. Additionally, there was a commercially available enzyme that could efficiently recognize and digest the unmethylated CpG-containing region. A MSRE-ddPCR probe assay for this CpG site was then designed (**Supplementary Fig. 2a**). The assay performed linearly ($R = 0.98$, $p < 0.00001$) on undigested methylated and unmethylated DNA samples (**Supplementary Fig. 2b**). Enzyme and substrate titrations were performed using artificially methylated and unmethylated DNA as well as non-tumor tissue derived DNA (**Supplementary Fig. 2c, d and e**). The ß-values, indicating the level of methylation at cg03287111 (a ratio between the methylated fraction and the overall signal intensity and ranges from between 0 and 1, where 0 is completely unmethylated and 1 is completely methylated) in tumor from two independent studies is shown in **Supplementary Fig. 2f and** g. In early stage tumor-derived DNA samples, hypermethylation was observed in tumor samples (Fig. 4**a**) compared with non-tumor lung tissue. Similarly, hypermethylation was observed in the corresponding plasma-derived cfDNA compared with cfDNA from healthy blood donors (Fig. 4**b**). Samples with higher tumor DNA methylation tend to have higher plasma DNA methylation (Fig. 4**c**). An AUC of 0.94 was achieved for early stage patients and 0.96 for late stage patients (Fig. 4**d and e**). Hypermethylation was equally detected in patients with undetectable or no tumor-reported genetic alterations, supporting the strength of cfDNA methylation as a complementary approach for monitoring tumor molecular dynamics.

^{meth}cfDNA kinetics and clinical outcome

We performed long-term serial ^{meth}cfDNA analysis on 17 advanced

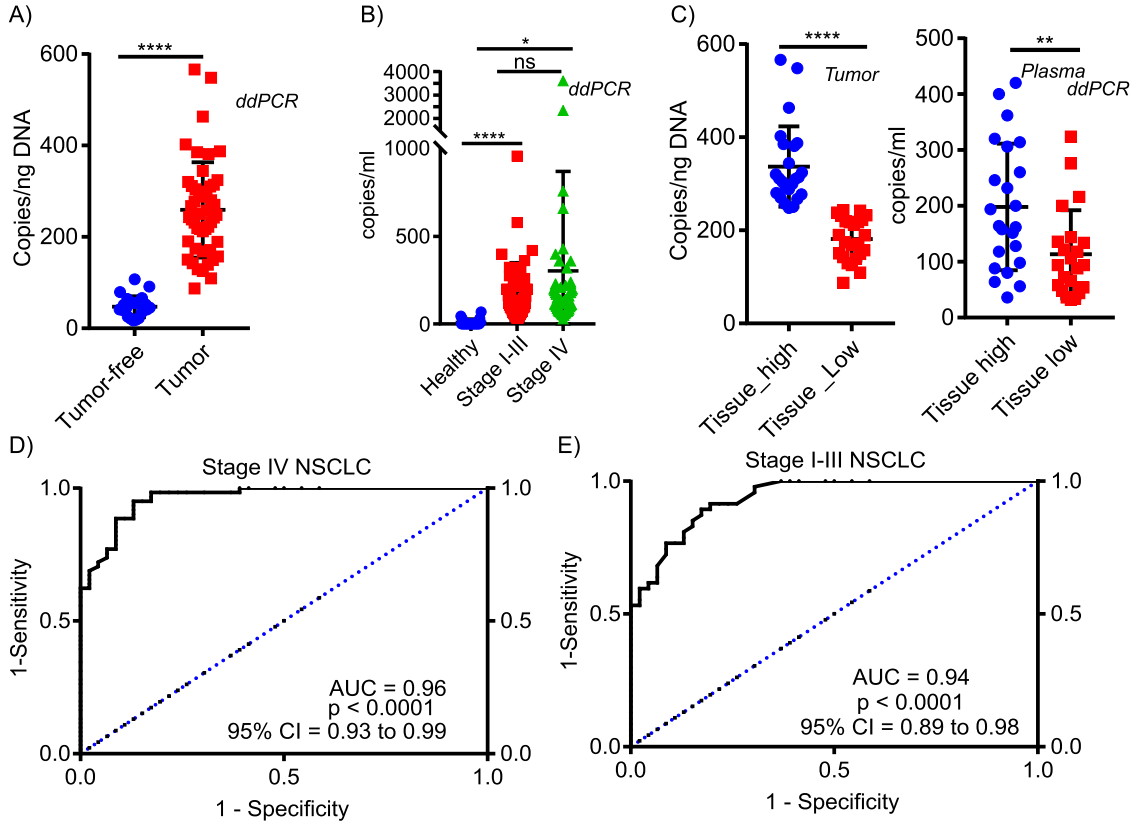

Fig. 4.. ^{meth}cfDNA allows for disease detection in early and late stage disease. A scatter plot showing the amount of DNA detected by ddPCR in MSRE-treated DNA from tumor (red, $n = 48$) and non-tumor (blue, $n = 22$) lung tissue. The same amount of tissue-derived DNA was used for both the tumor and tumor-free samples. The methylated DNA copy number was normalized to the total amount of input DNA. (**B**) A scatter plot showing the amount of DNA detected by ddPCR in MSRE-treated cfDNA from healthy blood donor (blue, $n = 39$) early stage NSCLC (red, $n = 48$) and late stage NSCLC samples (green, $n = 61$). cfDNA was isolated from 1 ml of plasma and the same volume of eluted DNA was used in the digestion/ddPCR reaction. The methylated DNA copy number is expressed per ml of plasma used for cfDNA isolation. (**C**) Scatter plots showing the stratification of early stage patients into high and low methylated groups based on median methylation levels in tumor DNA (left panel) and the abundance of methylated cfDNA from the same patients from the high and low groups (right panel). (**D**) A receiver operator characteristic curve showing the sensitivity and specificity performance of methylated cfDNA on late stage NSCLC patients. (**E**) A receiver operator characteristic curve showing the sensitivity and specificity performance of methylated cfDNA on early stage NSCLC patients. The scatter plots show the mean methylated cfDNA copy number per ml of plasma and the standard deviation. (For interpretation of the references to color in this figure legend, the reader is referred to the web version of this article).

stage NSCLC cases (40 samples). Radiological imaging and ^{meth}cfDNA profiles between baseline and follow-up samples was analyzed. Decrease in ^{meth}cfDNA concentration between baseline and first follow-up was associated with decrease in tumor volume (Fig. 5**a**) meanwhile a stable or increased ^{met}cfDNA kinetic showed a mixed response in tumor surface area profile between both time points (Fig. 5**b**). Two patients (patients #4 and patient #5) with no tumor-reported genetic alteration or with a cfDNA undetectable tumor-reported *KRAS* mutation could be monitored by cfDNA methylation (Fig. 5**c and d**). High Baseline ^{meth}cfDNA levels were associated with better progression-free survival but not with overall survival for the CpG site under investigation (Fig. 6a and b),

Discussion

We investigated the utility of combined circulating cell-free DNA analysis and CT-based imaging for treatment surveillance in lung cancer using next-generation sequencing, radiological imaging and ddPCR. Patient samples were collected during routine clinical visits to simulate a real-life situation. We included patients with tumor-confirmed driver molecular alteration. Molecular alterations in tumor tissue were scored using a custom generead V2 panel, while either next-generation sequencing (AVENIO) or ddPCR were used to analyze cfDNA mutation. Concomitantly, we developed a MSRE-based ddPCR method for cfDNA/tDNA methylation analysis.

We found 62.5% positive concordance between AVENIO-reported baseline cfDNA variants and the corresponding tumor tissue variant, which is similar to previous reports [26,27]. Increasing the input cfDNA amount may increase the concordance rate by increasing the number of genome equivalents. Resistance-mediating mutations (p.T790M) were found in some baseline cfDNA samples but not in the corresponding tumor tissue. Differences in tumor clone composition may explain such discrepancies [28,29]. Tumor heterogeneity may affect tumor but not plasma DNA [30] and such mutations have been reported in cfDNA from NSCLC patients [31,32]. Concordance between tumor-reported variants and baseline cfDNA variants called by ddPCR ranged from 50 to 100%, depending on the gene under investigation. Serial ctDNA kinetics reflected tumor dynamics in some but not all lesions in 2/3 patients monitored by ddPCR, meanwhile there was a perfect match in the ctDNA profile and tumor dynamics in 1/3 patients. Tumor architectural differences or the acquisition of novel mutations during cancer cell migration might in part explain such observations [33–35]. Taken together, these finding suggest that ctDNA mutational profiling alone might not be sufficient to monitors multiple lesions. To complement ctDNA we evaluated cfDNA methylation. ctDNA methylation analysis was proven to be useful for early disease detection and screening of colorectal cancer [36]. MSRE-ddPCR has been shown to be well suited for targeted methylation analysis [37–39].

Using MSRE-ddPCR, we demonstrated hypermethylation in plasma and tumor DNA. This is in line with reports where ^{meth}cfDNA has been reported to have strong diagnostic value in cancer [36,40–42]. ^{meth}cfDNA kinetics between baseline and first reassessment recapitulated the tumor dynamics in patients who responded to treatment. Heterogeneous ^{meth}cfDNA profiles were observed in non-responders. Here, we speculate a possible contribution from CT-undetectable lesions. Taken together, panel cfDNA sequencing coupled with ^{meth}cfDNA analysis can broaden the spectrum of eligible patients, while informing on lesions undetectable by CT and biological disease progression.

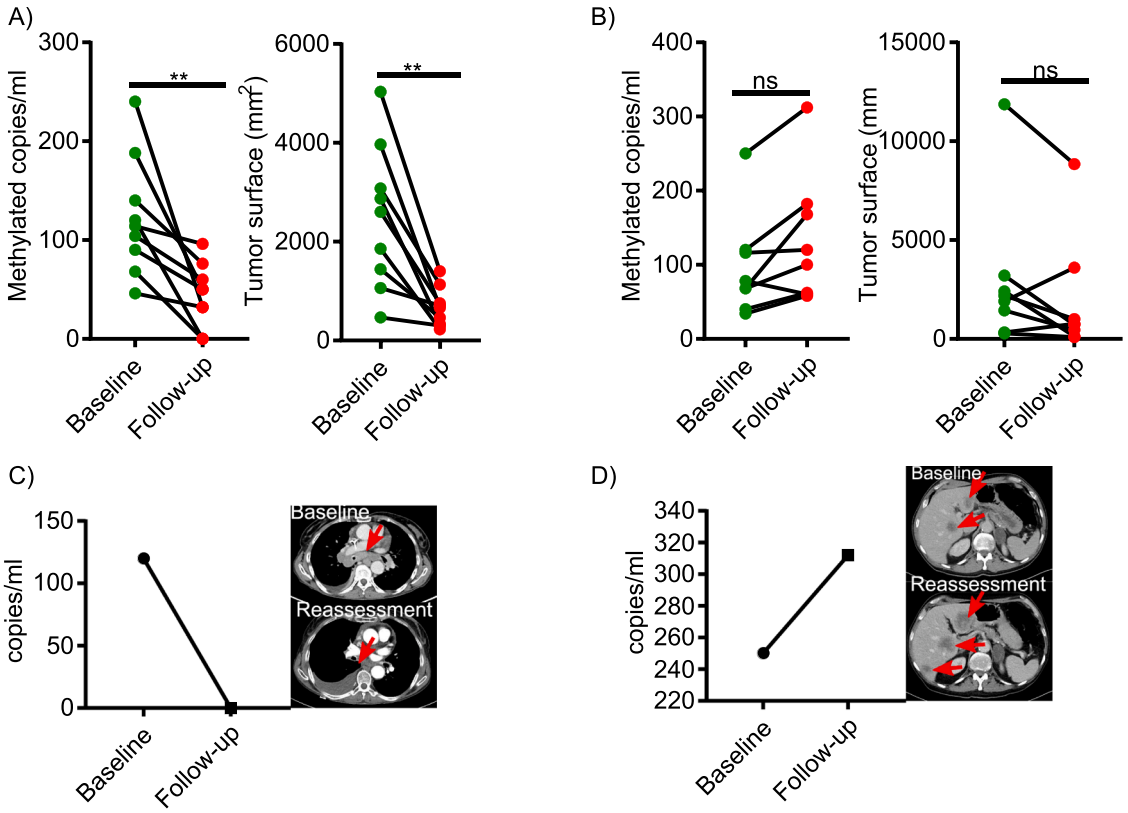

Fig. 5.. MSRE-coupled with ddPCR can be used for early detection and monitoring of NSCLC patients during treatment.(A) A profile plot showing the profile of methylated cfDNA (^{meth}cfDNA) between baseline and follow-up for patients whose ^{meth}cfDNA decreased between baseline and follow-up (left panel) and the tumor surface profile for baseline and follow-up time points for the same patients (right panel). (B) A profile plot showing the ^{meth}cfDNA profile between baseline and follow-up for patients whose ^{meth}cfDNA increased or remained stable between baseline and follow-up (left panel) and the tumor surface profile for baseline and follow-up time points for the same patients (right panel). (C) A representative profile plot and CT-image of a patient with decreased ^{meth}cfDNA between baseline and follow-up. (D) A representative profile plot and CT-image of a patient with increased or stable ^{meth}cfDNA profile between baseline and follow-up.

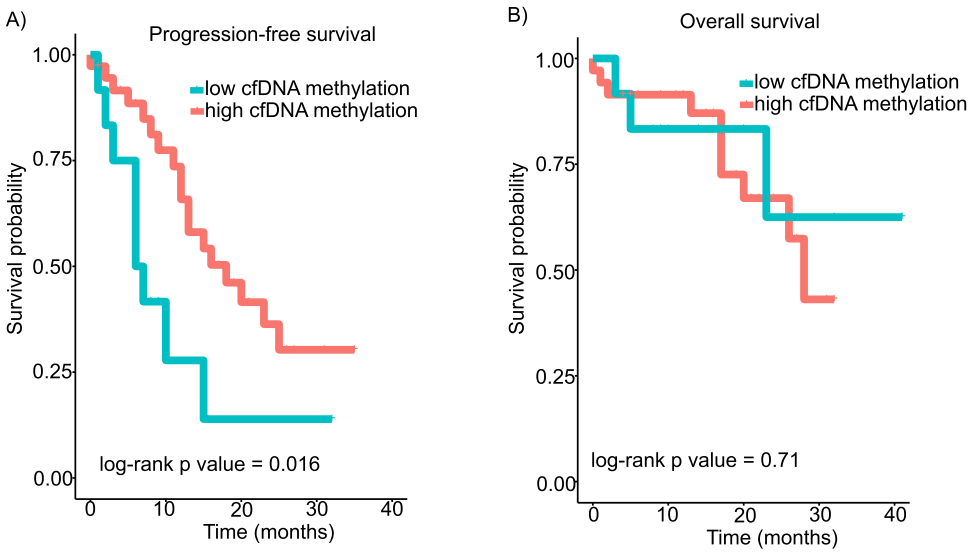

Fig. 6. High baseline methcfDNA are associated with better progression-free but not over all survival. Progression-free survival here is considered as the time from treatment initiation until disease progression or cancer-related death. Due to limited patient numbers, the therapies are not seperated.

Funding Information

This work was funded by a European Transcan-2 project CEVIR and the German Cancer Consortium (DKTK). S.S.L. was partially supported by the Deutsche Forschungsgemeinschaft (DFG, German Research Foundation)—SI 1549/3–1 and RO 3577/7–1 (KFO 337)

CRediT authorship contribution statement

Martin Metzenmacher: Investigation, Resources, Data curation, Writing – review & editing, Writing – original draft. **Balazs Hegedüs:** Investigation, Resources, Writing – original draft, Writing – review & editing. **Jan Forster:** Formal analysis, Writing – original draft, Writing – review & editing. **Alexander Schramm:** Resources, Writing – original draft, Writing – review & editing. **Peter A. Horn:** Resources, Writing – original draft, Writing – review & editing. **Christoph A. Klein:** Resources, Project administration, Writing – original draft, Writing – review & editing. **Nicola Bielefeld:** Resources, Project administration, Investigation, Writing – original draft, Writing – review & editing. **Till Ploenes:** Investigation, Resources, Writing – original draft, Writing – review & editing. **Clemens Aigner:** Resources, Writing – original draft, Writing – review & editing. **Dirk Theegarten:** Investigation, Resources, Writing – original draft, Writing – review & editing. **Hans-Ulrich Schildhaus:** Writing – original draft, Writing – review & editing. **Jens T. Siveke:** Resources, Writing – original draft, Writing – review & editing. **Martin Schuler:** Supervision, Funding acquisition, Conceptualization, Project administration, Writing – original draft, Writing – review & editing. **Smiths S. Lueong:** Conceptualization, Methodology, Investigation, Formal analysis, Writing – original draft, Project administration, Writing – original draft, Writing – review & editing.

CRediT authorship contribution statement

Martin Metzenmacher: Investigation, Resources, Data curation, Writing – review & editing, Writing – original draft. **Balazs Hegedüs:** Investigation, Resources, Writing – original draft, Writing – review & editing. **Jan Forster:** Formal analysis, Writing – original draft, Writing – review & editing. **Alexander Schramm:** Resources, Writing – original draft, Writing – review & editing. **Peter A. Horn:** Resources, Writing – original draft, Writing – review & editing. **Christoph A. Klein:** Resources, Project administration, Writing – original draft, Writing – review & editing. **Nicola Bielefeld:** Resources, Project administration, Investigation, Writing – original draft, Writing – review & editing. **Till Ploenes:** Investigation, Resources, Writing – original draft, Writing – review & editing. **Clemens Aigner:** Resources, Writing – original draft, Writing – review & editing. **Dirk Theegarten:** Investigation, Resources, Writing – original draft, Writing – review & editing. **Hans-Ulrich Schildhaus:** Writing – original draft, Writing – review & editing. **Jens T. Siveke:** Resources, Writing – original draft, Writing – review & editing. **Martin Schuler:** Supervision, Funding acquisition, Conceptualization, Project administration, Writing – original draft, Writing – review & editing. **Smiths S. Lueong:** Conceptualization, Methodology, Investigation, Formal analysis, Writing – original draft, Project administration, Writing – original draft, Writing – review & editing.

Declaration of Competing Interest

MM received honoraria from Boehringer Ingelheim, BMS, MSD, Roche and Takeda. All other authors declare no conflict of interest

Acknowledgments

We are thankful to the West German Biobank Essen for sample collection and the laboratory of Prof. Dr. med. Nils von Neuhoff for infrastructural support. We thank Eva Gottstein for the FFPE DNA isolation. We acknowledge support by the Open Access Publication Fund of the University of Duisburg-Essen.

Supplementary materials

Supplementary material associated with this article can be found, in the online version, at doi:10.1016/j.tranon.2021.101279.

References

[1] F. Bray, et al., Global cancer statistics 2018: GLOBOCAN estimates of incidence and mortality worldwide for 36 cancers in 185 countries, CA Cancer J. Clin. 68 (6) (2018) 394–424.

[2] Global Burden of Disease Cancer, C., The global burden of cancer 2013, JAMA Oncol. 1 (4) (2015) 505–527.

[3] R.L. Siegel, K.D. Miller, A. Jemal, Cancer statistics, 2019, CA Cancer J. Clin. 69 (1) (2019) 7–34.

[4] S. Blandin Knight, et al., Progress and prospects of early detection in lung cancer, Open Biol. 7 (9) (2017).

[5] P. Goldstraw, et al., The IASLC lung cancer staging project: proposals for revision of the TNM stage groupings in the forthcoming (Eighth) edition of the TNM classification for lung cancer, J. Thorac. Oncol. 11 (1) (2016) 39–51.

[6] C.J. Hoekstra, et al., Methods to monitor response to chemotherapy in non-small cell lung cancer with 18F-FDG PET, J. Nucl. Med. 43 (10) (2002) 1304–1309.
[7] D. Planchard, et al., Metastatic non-small cell lung cancer: ESMO Clinical Practice Guidelines for diagnosis, treatment and follow-up, Ann. Oncol. 29 (2018) 192–237.
[8] N. Hanna, et al., Systemic therapy for stage IV non-small-cell lung cancer: American society of clinical oncology clinical practice guideline update, J. Clin. Oncol. 35 (30) (2017) 3484. -+.
[9] A.F. Farago, E.L. Snyder, T. Jacks, SnapShot: lung cancer models, Cell 149 (1) (2012) 246. -246 e1.
[10] C. Iragavarapu, et al., Novel ALK inhibitors in clinical use and development, J. Hematol. Oncol. 8 (2015) 17.
[11] M. Fukuoka, et al., Biomarker analyses and final overall survival results from a phase III, randomized, open-label, first-line study of gefitinib versus carboplatin/paclitaxel in clinically selected patients with advanced non-small-cell lung cancer in Asia (IPASS), J. Clin. Oncol. 29 (21) (2011) 2866–2874.
[12] M.S. Tsao, et al., Erlotinib in lung cancer - molecular and clinical predictors of outcome, N. Engl. J. Med. 353 (2) (2005) 133–144.
[13] J.Y. Douillard, et al., Molecular predictors of outcome with gefitinib and docetaxel in previously treated non-small-cell lung cancer: data from the randomized phase III INTEREST trial, J. Clin. Oncol. 28 (5) (2010) 744–752.
[14] M.J. Overman, et al., Use of research biopsies in clinical trials: are risks and benefits adequately discussed? J. Clin. Oncol. 31 (1) (2013) 17–22.
[15] J.C.M. Wan, et al., Liquid biopsies come of age: towards implementation of circulating tumour DNA, Nat. Rev. Cancer 17 (4) (2017) 223–238.
[16] F. Diehl, et al., Circulating mutant DNA to assess tumor dynamics, Nat. Med. 14 (9) (2008) 985–990.
[17] R.H. Xu, et al., Circulating tumour DNA methylation markers for diagnosis and prognosis of hepatocellular carcinoma, Nat. Mater. 16 (11) (2017) 1155–1161.
[18] J.Y. Douillard, et al., Gefitinib treatment in EGFR mutated caucasian NSCLC: circulating-free tumor DNA as a surrogate for determination of EGFR status, J. Thorac. Oncol. 9 (9) (2014) 1345–1353.
[19] D. Roy, et al., Cell-free circulating tumor DNA profiling in cancer management, Trends Mol. Med. 27 (10) (2021) 1014–1015.
[20] D.T. Dhruvajyoti Roy, Z. Lianghong, L. Dan, G. Li, M. Li, K. Zhang, R.A. Van Etten, Circulating cell-free DNA methylation assay: towards early detection of multiple cancer types, Cancer Res. 79 (13) (2019).
[21] C. Bettegowda, et al., Detection of circulating tumor DNA in early- and late-stage human malignancies, Sci. Transl. Med. 6 (224) (2014), 224ra24.
[22] L. Vrba, et al., DNA methylation biomarkers discovered in silico detect cancer in liquid biopsies from non-small cell lung cancer patients, Epigenetics 15 (4) (2020) 419–430.
[23] D. Roy, M. Tiirikainen, Diagnostic power of DNA methylation classifiers for early detection of cancer, Trends Cancer 6 (2) (2020) 78–81.
[24] T. Sing, et al., ROCR: visualizing classifier performance in R, Bioinformatics 21 (20) (2005) 3940–3941.
[25] L. Ding, et al., Somatic mutations affect key pathways in lung adenocarcinoma, Nature 455 (7216) (2008) 1069–1075.
[26] C.C. Bieg-Bourne, R. Okamura, R. Kurzrock, Concordance between TP53 alterations in blood and tissue: impact of time interval, biopsy site, cancer type and circulating tumor DNA burden, Mol Oncol 14 (6) (2020) 1242–1251.
[27] J. Jiang, et al., Concordance of genomic alterations by next-generation sequencing in tumor tissue versus cell-free DNA in stage I-IV non-small cell lung cancer, J. Mol. Diagn. 22 (2) (2020) 228–235.
[28] K.M. Giessler, et al., Genetic subclone architecture of tumor clone-initiating cells in colorectal cancer, J. Exp. Med. 214 (7) (2017) 2073–2088.
[29] Y.C.S. Ramon, et al., Clinical implications of intratumor heterogeneity: challenges and opportunities, J. Mol. Med. 98 (2) (2020) 161–177 (Berl).
[30] J. Nong, et al., Circulating tumor DNA analysis depicts subclonal architecture and genomic evolution of small cell lung cancer, Nat. Commun. 9 (1) (2018) 3114.
[31] C. Vollbrecht, et al., Validation and comparison of two NGS assays for the detection of EGFR T790M resistance mutation in liquid biopsies of NSCLC patients, Oncotarget 9 (26) (2018) 18529–18539.
[32] S.R. Fairclough, et al., Identification of osimertinib-resistant EGFR L792 mutations by cfDNA sequencing: oncogenic activity assessment and prevalence in large cfDNA cohort, Exp. Hematol. Oncol. 8 (2019) 24.
[33] W. Schrijver, et al., Mutation profiling of key cancer genes in primary breast cancers and their distant metastases, Cancer Res. 78 (12) (2018) 3112–3121.
[34] G. Liu, et al., Genomics alterations of metastatic and primary tissues across 15 cancer types, Sci. Rep. 7 (1) (2017) 13262.
[35] A. Heyde, et al., Consecutive seeding and transfer of genetic diversity in metastasis, Proc. Natl. Acad. Sci. U. S. A., 116 (28) (2019) 14129–14137.
[36] H. Luo, et al., Circulating tumor DNA methylation profiles enable early diagnosis, prognosis prediction, and screening for colorectal cancer, Sci. Transl. Med. 12 (524) (2020).
[37] C. De Rop, et al., Methylation analysis of MLH1 using droplet digital PCR and methylation sensitive restriction enzyme, Ann. Oncol. 30 (2019) 576. -576.
[38] K. Hashimoto, et al., Improved quantification of DNA methylation using methylation-sensitive restriction enzymes and real-time PCR, Epigenetics 2 (2) (2007) 86–91.
[39] M. Ioannides, et al., Development of a new methylation-based fetal fraction estimation assay using multiplex ddPCR, Mol. Genet Genom. Med. 8 (2) (2020) e1094.
[40] J.S. Bhangu, et al., Circulating free methylated tumor DNA markers for sensitive assessment of tumor burden and early response monitoring in patients receiving systemic chemotherapy for colorectal cancer liver metastasis, Ann. Surg. 268 (5) (2018) 894–902.
[41] W.W. Tang, et al., Correlation between ctDNA methylation and CEA in colorectal cancer, Ann. Oncol. 29 (2018).
[42] K. Misawa, et al., Identification of novel methylation markers in HPV-associated oropharyngeal cancer: genome-wide discovery, tissue verification and validation testing in ctDNA, Oncogene 39 (24) (2020) 4741–4755.